17

Detection of superposition of twisted beams under noise with the use of artificial neural networks

© V.V. Chechetkin[1], A.V. Semenova[2,3], M.B. Chernyaeva[1,2], V.L. Vaks[1,2,3]

[1] Lobachevsky State University of Nizhny Novgorod (UNN)
Nizhny Novgorod, Russia
[2] The Institute for Physics of Microstructures of the Russian Academy of Sciences (IPM RAS),
Afonino, Russia
[3] Ioffe Institute, St. Petersburg, Russia

e-mail: elena@ipm.sci-nnov.ru

Received June 02, 2025
Revised August 22, 2025
Accepted September 03, 2025

Twisted beams with non-zero orbital angular momentum projection onto the direction of motion have attracted sufficient interest in recent years. Such beams with non-zero orbital angular momentum can be used in wireless communication networks to improve efficiency and throughput.The work is aimed to evaluate the efficiency of the artificial neural network for the recognition of the superposition of twisted beam under conditions of noise in the receiving channel, as well as variations in the orientation and spatial positioning of images of intensity profiles of the superposition of two twisted beams. The results could be applied for analysis of the potential of the artificial networks in wireless optical communications.

Keywords: Laguerre-Gaussian beams, orbital angular momentum, topological charge, optical communications, free space optics, optical angular momentum shift-keying, multiplexing, machine learning, convolutional neural networks, LeNet.

DOI: 10.61011/EOS.2025.09.62310.8233-25

Introduction

The work is devoted to the study of a phenomenon known as scalar optical vortices or twisted photons (i.e., photons possessing a nonzero projection of orbital angular momentum (OAM) onto the direction of propagation), as well as the task of recognizing optical vortices using neural networks.

Rapid technical progress demands increased bandwidth, higher speed, ease of installation, and reliability of data transmission networks. Free-space optical communication (FSO), as a new communication technology, meets these requirements. Information in FSO systems is „encoded“ and transmitted by modulating certain electromagnetic wave parameters.

It is known that electromagnetic waves carry energy, momentum, and angular momentum. Early works [1–3] considered transferring the spin angular momentum of electromagnetic waves to mechanical systems. However, photon angular momentum comprises not only spin but also an orbital component. Individual photons and electromagnetic wave beams corresponding to eigenvalues of the operator projecting orbital angular momentum on the propagation direction are called twisted beams or scalar optical vortices. Since the OAM of an electromagnetic wave beam depends on the phase, intensity, or polarization distribution in the beam's cross-section, forming an optical vortex requires highly coherent radiation and optical systems that transform the beam with high precision. Thus, detailed study of such beams became possible only after lasers appeared. Great interest in optical vortices arose in 1992 after the publication by Allen et al. [4]. In this article, the authors demonstrated that laser beams with helical wavefronts (Fig. 1) possess definite orbital angular momentum and proposed methods for generating and detecting such beams.

Such beams include exact and approximate solutions of the Helmholtz equation in cylindrical coordinates: Bessel beams, Bessel-like beams, Laguerre-Gaussian (LG) beams [5]. All sufficiently well approximate photon fluxes in eigenstates of the OAM operator projection l [5], where $l = 0, \pm 1, \pm 2 \ldots$. The quantity l is also known as the topological charge or winding number [5]. Note that the OAM projection can also be nonzero for spherical waves or beams with specific polarization distributions [6]. However, this work focuses on recognizing superpositions of optical vortices potentially useful in communication systems. Therefore, primary attention will be given to Laguerre-Gaussian beams: unlike spherical waves, they have a definite propagation direction, and unlike true Bessel beams, they carry finite power and can be formed in real setups. It should be noted that Bessel-like beams [5] may also be of interest for communication systems, but their detailed consideration is beyond the scope of this work.

Thus, OAM eigenstates defined by different topological charge values are mutually orthogonal. The number of such states, like the topological charge itself, is theoretically unlimited. Thus, OAM is an additional degree of freedom allowing increased photon information capacity.

Several promising optical communication technologies rely on transmitting information via optical vortices. Studies show that optical vortices enable high data transmission rates and can be used to enhance network efficiency and throughput, including in FSO systems. Research on communication channels using OAM beams is conducted from millimeter to optical ranges. In a communication channel using four multiplexed OAM beam modes and two polarizations, a transmission rate of 32 Gbit/s at 28 GHz was achieved, while combining OAM multiplexing with conventional spatial multiplexing in a millimeter-range (28 GHz) communication line demonstrated 100 Gbit/s. In the THz range, an experimental system was demonstrated combining polarization-division multiplexing (PDM), frequency-division multiplexing (FDM), and OAM, enabling multiplexing of 8 data channels with a total data rate of 32 Gbit/s at a carrier frequency of$\sim$ 300 GHz [7]. Higher data transmission rates have been achieved in the optical range. For example, in [8], a data rate of 1.6 Tbit/s was achieved over 1.1 km of optical fiber. In another study [9], using optical vortices enabled data rates up to 2.56 Tbit/s. Developing OAM-based communication channels operating across various frequency ranges (acoustic, radio, millimeter, terahertz, optical) requires finding compromises between beam divergence effects and interactions of propagating electromagnetic radiation with the medium.

To determine a beam's OAM, various interference and diffraction methods are typically used. For example, interference between a plane wave and an optical vortex produces a fringe system where one fringe branches like a „fork"; the structure of this branching point is determined by the beam's topological charge. Interference between beams with equal-magnitude but opposite-sign topological charges forms a characteristic multi-petaled structure. However, as the topological charge value increases, such interference patterns become difficult to distinguish. Using neural networks for recognizing such structures is promising; for instance, in studying the evolution of spatial mode structures during propagation over 143 km through an atmospheric channel, interference patterns from superpositions of various modes were distinguished using an artificial neural network [10]. For practical application of optical vortices in communication systems, it is necessary to investigate the influence of real conditions (turbulence, noise) that introduce signal distortions during channel transmission on signal reception. Machine learning methods using convolutional neural networks, exemplified by modeling signal propagation where encoding was performed using optical vortices in free space under simulated atmospheric turbulence, as well as Gaussian noise, followed by demultiplexing based on recognition of multiplexed OAM beam intensities, are presented in [11]. In [12], demultiplexing based on recognition of multiplexed OAM beam intensities under atmospheric turbulence was implemented via a hybrid opto-electronic neural network, employing a single convolutional layer to perform the complete Fourier optics convolution operation integrated with the current optical setup, providing an advantage over neural networks with more complex structures, since convolution remains the primary computational component of convolutional neural networks, with lower computational resource expenditure.

It should be noted that, according to Shannon's theorem, noise in communication systems not only determines receiver sensitivity to weak signals but also limits the information transmission rate. The aim of this work is to solve the problem of recognizing superpositions of optical vortices using neural networks for their potential use in communications, as well as to evaluate the neural network's performance efficiency under noise conditions in the receiving channel, and under variations in orientation and spatial positioning of intensity profile images of the superposition of two optical vortices.

Theoretical Information on Optical Vortices

It is known [13] that the wave equation in the paraxial approximation is a simplified form of the Helmholtz equation (1):

$$\Delta u + k^2 u = 0, \tag{1}$$

where $k = \omega/c$ is the wave number, Δ is the Laplacian operator. In the paraxial approximation, the wave propagates at small angles relative to the propagation axis (e.g., the z axis), and the wave equation reduces to the following expression:

$$\left(\frac{\partial^2}{\partial x^2} + \frac{\partial^2}{\partial y^2}\right)u + 2jk\,\frac{\partial u}{\partial z} = 0. \tag{2}$$

The solution to the wave equation (2) is usually represented as an expansion in eigenmodes. Several equivalent sets of eigenmodes exist. For describing optical vortices, Laguerre-Gaussian solutions are used. The distribution of the transverse component of the magnetic field's vector potential in Laguerre-Gaussian beams in cylindrical coordinates is as follows [14]:

$$u_{p,l}(r, \varphi, z) = \sqrt{\frac{2p!}{\pi w^2(z)(p+|l|)!}}\left[\frac{r\sqrt{2}}{w(z)}\right]^{|l|}$$
$$\times L_p^{|l|}\left(\frac{2r^2}{w^2(z)}\right)\exp\left[\frac{-r^2}{w^2(z)}\right]\exp\left[\frac{jkr^2 z}{2(z^2+z_R^2)}\right]$$
$$\times \exp\left[-j(2p+|l|+1)\tan^{-1}\left(\frac{z}{z_R}\right)\right]\exp(jl\varphi), \tag{3}$$

where $w(z) = w_0[(z^2 + z_R^2)/z_R^2]^{1/2}$ is the beam radius, w_0 is the minimum beamwidth, z_R is the Rayleigh length, k is the wave number, p is a non-negative integer (radial index), $l \in Z$ is the topological charge, $L_p^{|l|}(x)$ is the generalized Laguerre polynomial, which can be computed by the formula:

$$L_p^{|l|}(x) = \frac{x^{-|l|}e^x}{p!}\,\frac{d^p}{dx^p}(e^{-x}x^{p+|l|}).$$

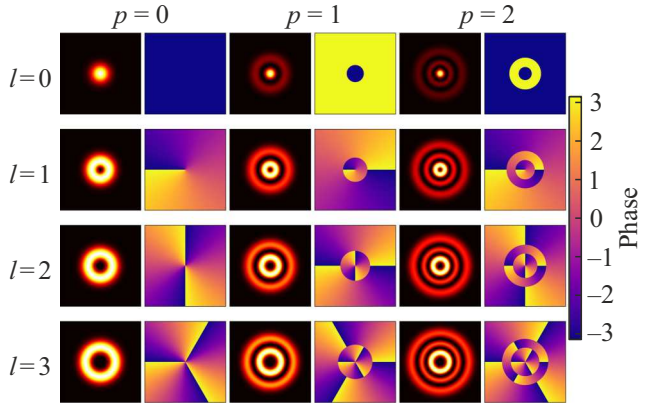

Figure 1. Distribution of intensity and phase of various Laguerre-Gaussian modes at $z = 0$.

Precisely the factor $\exp(il\varphi)$ in (3), containing the azimuthal phase dependence, forms the helical wavefront. Figure 1 shows the modeled distribution of phase and intensity of Laguerre-Gaussian beams at various values of the topological charge l and radial index p in the plane $z = 0$. The modeling was performed using the Python programming language with the *NumPy* [15] and *Matplotlib* libraries [16].

Modulation Using OAM

A key element in developing a communication channel is the selection of modulation methods, which are constantly being improved. One promising method is modulation with orbital angular momentum (OAM-SK, *orbital angular momentum-shiftkeying*).

In an optical communication system, each OAM mode, corresponding to its topological charge l can represent a unique symbol. By assigning a specific bit sequence to each unique value of l a signal can be transmitted that carries information encoded using individual OAM modes. For example:

1) $l = 0$ corresponds to the bit sequence „00“,
2) $l = 1$ corresponds to „01“,
3) $l = -1$ corresponds to „10“,
4) $l = 2$ corresponds to „11“.

In this case, each OAM mode carries 2 bits of information. Accordingly, the more different OAM states are used, the more information can be encoded in each photon. For example, using 16 OAM states, each beam can carry 4 bits of information.

Thus, OAM-SK can provide high data transmission rates by utilizing the unique properties of beams with non-zero OAM and their associated topological charge value l.

In the case of superposition of two optical vortices, the received signal has a specific intensity profile. For processing such a signal in the receiving system, neural networks can be used [10]. However, noise present in real conditions distorts the received image. The presented work

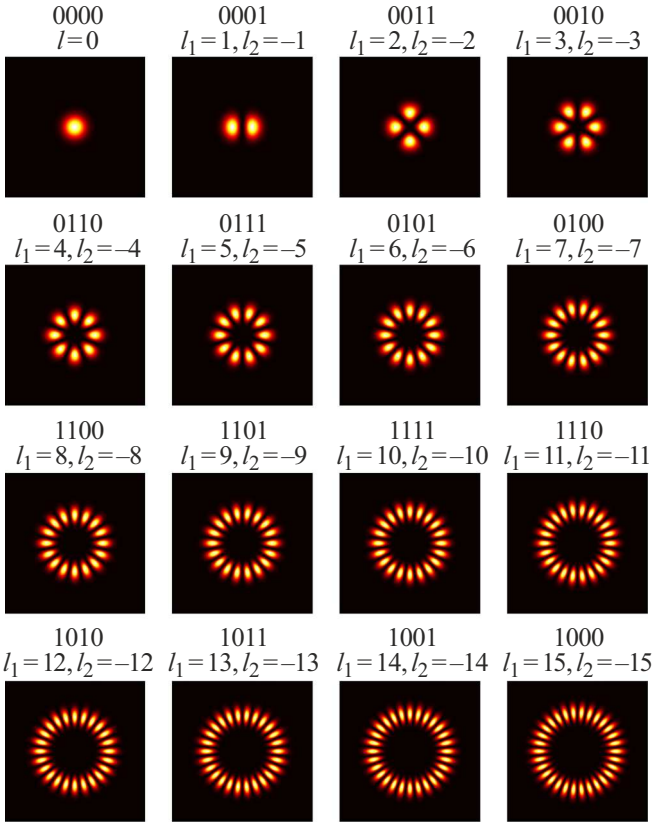

Figure 2. Intensity profiles of the superposition of two optical vortices with topological charges l_1 and l_2 ($l_1 = -l_2$) and possible corresponding bit sequences. Each superposition corresponds to its class.

considers the application of a convolutional neural network for processing the superposition of two optical vortices and evaluating the effectiveness of its application in the presence of noise in the receiving channel. Convolutional neural networks are capable of working with complex and noisy data, which distinguishes them from traditional methods (e.g., correlation computation) that are less reliable with distorted data.

Neural networks can be used to classify input data. A convolutional neural network outputs the probability of assigning input data to each class; the class with the highest probability is considered the model's prediction. In our case, each superposition of beams with topological charges l_1 and l_2 belongs to its class l ($l = l_1 = -l_2 = 0, 1, 2 \ldots 15$) i.e., there are 16 classes in total (Fig. 2).

Tools Used for Simulation

To achieve the goal, *Python* was chosen as the main programming language. The use of this language is justified by its simplicity, versatility, and extensive set of libraries that simplify development and allow solving a wide range of tasks.

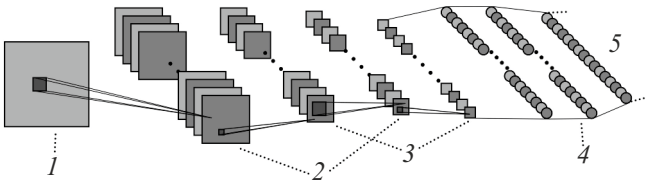

Figure 3. Architecture of the convolutional neural network *LeNet* [18]. *1* — input image, *2* — feature maps, *3* — subsampled feature maps, *4* — fully connected neural network, *5* — neural network output.

Modeling of optical vortices and training of the neural network (Fig. 3) was performed using the following libraries:

1) *NumPy* [15] — a library for computations in *Python*. It provides support for large multidimensional arrays and matrices, as well as a set of mathematical functions for efficient operations on these arrays.

2) *Matplotlib* [16] — a *Python*, library for creating high-quality static, animated, and interactive data visualizations. It offers extensive customization options and supports a wide range of graph types, such as line plots, histograms, scatter plots, and heatmaps.

3) *PyTorch* [17] — an open-source machine learning library. It is widely used for deep learning tasks due to its flexibility and ease of model modification. PyTorch provides extensive tools for tensor computations (similar to NumPy) and GPU support.

Dataset Preparation for Neural Network Training

In a typical convolutional neural network architecture, the input image passes through a series of layers that create feature maps. Feature maps are generated during convolution with a filter (matrix) designed or trained to detect a specific pattern in the input data (or feature map from the previous layer). The convolutional layer uses multiple filters, each creating its own feature map, thereby capturing a diverse set of features from the input. The neural network model used in this work is based on the *LeNet* architecture (Fig. 3) [18]. The *LeNet* architecture was originally developed for handwritten digit recognition. This model is relatively simple and consists of two convolutional layers, two max-pooling layers (downsampling used to reduce the spatial size of the input volume), and three fully connected neural network layers. The output layer of the neural network contains 16 neurons, each corresponding to one class.

One of the problems in training neural networks is creating training and test datasets. Creating datasets of real labeled data for training is an extremely labor- and time-intensive process, so synthetic data are used for neural network training in most cases. Entire fields of research are devoted to creating algorithms for synthesizing training data, identifying possible problems, and increasing the realism of synthesized training data, for example [19,20]. Although synthetic data cannot account for all distorting factors present in real data, expanding and modifying the set of synthesized data by adding data constructed taking into account individual distortion causes (noise, image rotations, shifts, etc.) increases the realism of the training and test samples [20].

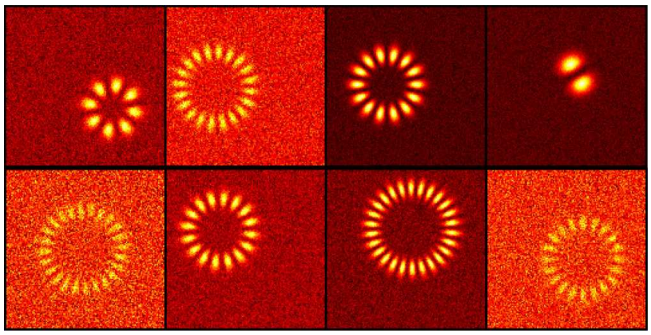

Figure 4. Examples of data used for training and testing the neural network.

Two large datasets were created for training: 48 000 images for training and 19 200 images for checking the model's effectiveness and reliability (test data) (Fig. 4). To ensure that the model generalizes well to data close to real ones and handles data variations, several data augmentation methods were applied to the images. In particular, additive white Gaussian noise was added to the images. The signal-to-noise ratio (SNR) varied from −15 dB to 15 dB, simulating various levels of signal distortion and ensuring good model performance under noise conditions. Additionally, to account for variations in orientation and spatial positioning, the images were subjected to random rotations and random shifts. Such additions allowed the model to train and adapt to a wide range of possible input data.

Results

Fig. 5 shows the principle of operation of the neural network in recognizing the superposition of optical vortices. The input is an image of the superposition of two optical vortices, and the output of the 16 neurons represents the probability of belonging to one of the classes. Accordingly, the neuron with the highest output value is considered the model's prediction.

Fig. 6 shows the neural network training process. The effectiveness of the neural network is characterized by the loss function, which determines the deviations of the model's predictions from the „true" predictions. In other words, the loss function tracks the degree of error in the neural network's output data. A simple example is the

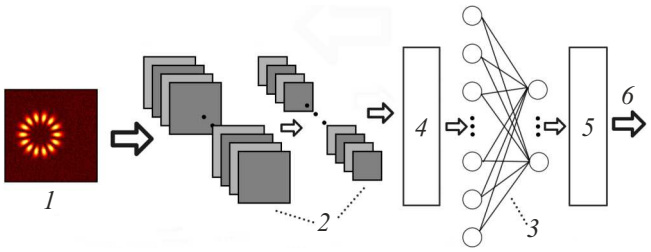

Figure 5. Neural network operation principle: *1* — input image; *2* — feature maps; *3* — fully connected neural network; *4* — vectorization; *5* — selection of neuron with maximum output value; *6* — determination of the received superposition (e.g., the 8th neuron corresponds to the superposition $l = \pm 7$) based on the selected neuron.

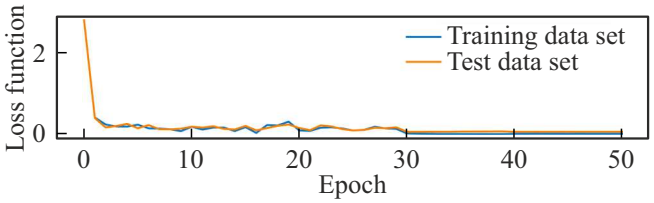

Figure 6. Neural network training process. The neural network output represents unnormalized probabilities of belonging to each class, so the loss function is dimensionless.

quadratic loss function:

$$E = \frac{1}{N}\sum_{i=0}^{N}(y_i - a_i)^2,$$

where N is the number of classes, y_i is the neural network output result, a_i is the expected result. For training the neural network in *PyTorch* cross-entropy (*CrossEntropyLossFunction*) [14] was used as the loss function, which is well-suited for classification tasks.

At the initial stages of training, the loss function should gradually decrease. This indicates that the model is beginning to learn and adjusts its weights based on the error. When the loss function stops changing significantly or reaches a plateau, it may indicate that the model has achieved a certain level of effectiveness, and further training will not yield significant improvements. In such a case, for example, if over 15–20 epochs (an epoch is one training cycle on the dataset) the loss function changes by no more than a small value (e.g., 0.01), training can be stopped. In our case, the training process took about 50 epochs.

The accuracy values of the trained model are high both on the training dataset (Fig. 7, *a*), and on the test dataset (Fig. 7, *b*), mainly in the range from 96.2 to 99.8%, indicating that the neural network performs well overall ($A_i = 100 \times \frac{M_i}{N_i}$ — accuracy for class $i = 0, 1 \ldots 15$, where M_i — number of correct predictions, N_i — sample size). This suggests that the model has learned the main patterns of the input data and generalized them.

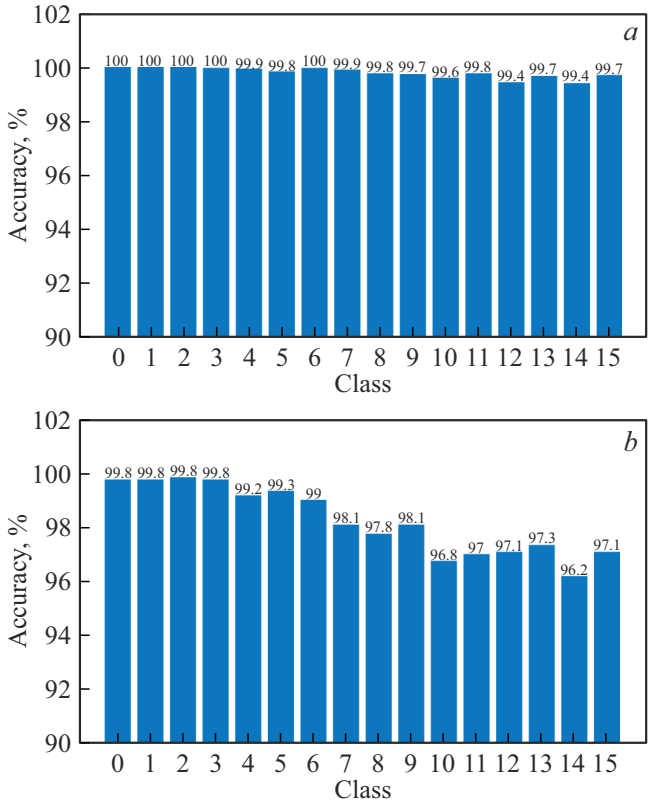

Figure 7. Network performance on training data (*a*) and test data (*b*).

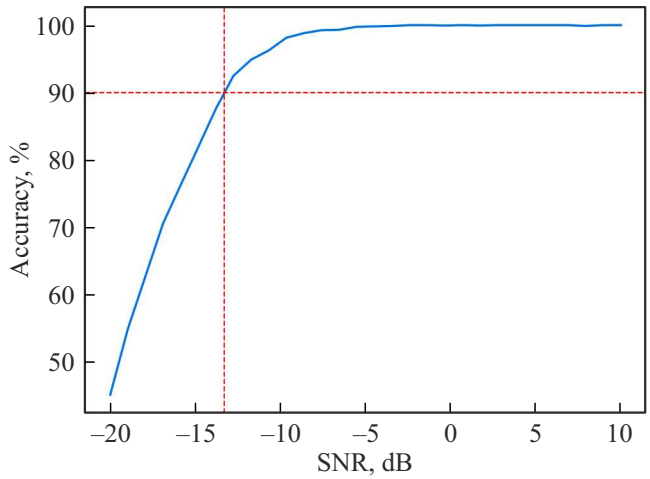

Figure 8. Network performance depending on SNR. Accuracy values were obtained by averaging 1600 realizations for each SNR value. Dashed lines mark the SNR boundary at which network accuracy reaches 90%.

It can be noted that the network performs worse with input data corresponding to higher topological charge values (classes with higher ordinal numbers). This can be explained by the fact that at such topological charge values, it is harder to recognize finer details in the intensity profile, especially under noise conditions. Thus, although

theoretically the maximum topological charge of a beam is unlimited, in practice the maximum possible topological charge value is determined by the noise level and the requirements for acceptable recognition error rates in a specific system.

Fig. 8 shows the network performance depending on SNR. It is evident that as SNR increases, the model works more accurately. From the graph in Fig. 8, it can be concluded that the neural network can operate effectively (its accuracy above 90%) at SNR values above −13 dB.

Conclusion

This work implemented a solution to the problem of recognizing the superposition of optical vortices using a convolutional neural network for their potential application in communications, and evaluated the effectiveness of this method under noise conditions.

The neural network used, based on the *LeNet* architecture, trained and tested on datasets of more than several tens of thousands of vortex superposition images with added additive white Gaussian noise, as well as subjected to random rotations and shifts, was able to adapt to the input data. Accuracy values were high both on the training (up to 99.8%) and test (up to 96.2%) datasets. In particular, testing of the trained model showed that it can effectively handle the task of recognizing optical vortex superpositions at SNR values above −13 dB. At such SNR values, recognition accuracy is above 90%.

It should be noted that the probability of misrecognition increases with increasing topological charge. Accordingly, although there are no theoretical limits on the topological charge, a practical limitation was found, determined by the SNR level and the acceptable classification error probability of a specific system. In a sense, this limitation follows from Shannon's theorem for an optical vortex communication system: for a given noise level, it determines the information capacity of a photon and, accordingly, the maximum possible information transmission rate. The obtained results can be used in further design of optical vortex-based communication systems.

Acknowledgments

The authors would like to thank E.G. Domracheva for productive discussion of the article materials.

Funding

This study was supported by the Russian Science Foundation, grant № 21-72-30020-P, https://rscf.ru/project/21-72-30020/.

Conflict of interest

The authors declare that they have no conflict of interest.

References

[1] A.I. Sadovsky. Uchenyya zapiski Imperatorskago Yur'evskago Universiteta, **1**, 1–126 (1899). (in Russian)
[2] J.H. Poynting. Proc. R. Soc. Lond. A, **82**, 560–567 (1909). DOI: 10.1098/rspa.1909.0060
[3] R.A. Beth. Phys. Rev., **50** (2), 115–125 (1936). DOI: 10.1103/PhysRev.50.115
[4] L. Allen, M.W. Beijersbergen, R.J.C. Spreeuw, J.P. Woerdman. Phys. Rev. A, **45** (11), 8185–8189 (1992). DOI: 10.1103/physreva.45.8185
[5] B.A. Knyazev, V.G. Serbo. Phys. Usp., **61**, 449–479 (2018). DOI: 10.3367/UFNr.2018.02.038306.
[6] X.-L. Wang, J. Chen, Y. Li, J. Ding. Phys. Rev. Lett., **105**, 253602 (2010).
[7] A.E. Willner, K. Pang, H. Song, K. Zou, H. Zhou. Appl. Phys. Rev., **8** (4), 041312 (2021). DOI: 10.1063/5.0054885
[8] N. Bozinovic, Y. Yue, Y. Ren, M. Tur, P. Kristensen, H. Huang, A.E. Willner, S. Ramachandran. Science, **340** (6140), 1545–1548 (2013). DOI: 10.1126/science.1237861
[9] J. Wang, J.-Y. Yang, I.M. Fazal, N. Ahmed, Y. Yan, H. Huang, Y. Ren, Y. Yue, S. Dolinar, M. Tur, A.E. Willner. Nat. Photonics, **6** (7), 488–496 (2012). DOI: 10.1038/nphoton.2012.138
[10] M. Krenn, J. Handsteiner, M. Fink, R. Fickler, R. Ursin, M. Malik, A. Zeilinger. Proc. Natl. Acad. Sci. USA, **113** (48), 13648–13653 (2016). DOI: 10.1073/pnas.1612023113
[11] T. Doster, A.T. Watnik. Appl. Opt., **56** (12), 3386–3396 (2017). DOI: 10.1364/AO.56.003386
[12] J. Ye, H. Kang, Q. Cai, Z. Hu, M. Solyanik-Gorgone, H. Wang, E. Heidari, Ch. Patil, M.-A. Miri, N. Asadizanjani, V. Sorger, H. Dalir. Commun. Phys., **7**, 105 (2024). DOI: 10.1038/s42005-024-01571-3
[13] H. Haus. *Volny i polya v optoelektronike*. Translated from English (Mir, M., 1988) (in Russian).
[14] A.M. Yao, M.J. Padgett. Adv. Opt. Photon., **3**, 161–204 (2011). DOI: 10.1364/AOP.3.000161
[15] C.R. Harris, K.J. Millman, S.J. van der Walt et al. Nature, **585**, 357–362 (2020). DOI: 10.1038/s41586-020-2649-2
[16] J.D. Hunter. CiSE, **9** (3), 90–95 (2007). DOI: 10.1109/MCSE.2007.55
[17] J. Ansel, E. Yang, H. He et al. In: ASPLOS '24: Proceedings of the 29th ACM International Conference on Architectural Support for Programming Languages and Operating Systems, **2**, 929–947 (2024). DOI: 10.1145/3620665.3640366
[18] R.C. Gonzalez, R.E. Woods. *Digital image processing*, 4th ed. (Global ed., Pearson Education, 2018).
[19] S.Yu. Pchelincev, M.A. Lyashkov, O.A. Kovalyova. Informacionno-upravlyayushchie sistemy, **3**, 9–19 (2022). (in Russian) DOI: 10.31799/1684-8853-2022-3-9-19
[20] A.V. Parasich, V.A. Parasich, I.V. Parasich. Informacionno-upravlyayushchie sistemy, **4**, 61–70 (2021). (in Russian) DOI: 10.31799/1684-8853-2021-4-61-70

Translated by J.Savelyeva